

# Thermal, mechanical, and rheological properties of micro-fibrillated cellulose-reinforced starch foams crosslinked with polysiloxane-based cross-linking agents

Mohammad Mahbubul Hassan\*, † Ian J. Fowler

*<sup>1</sup>Bioproduct and Fiber Technology Team, Lincoln Research Centre,  
AgResearch Limited, 1365 Springs Road, Lincoln, Canterbury 7647, New  
Zealand.*

## **Abstract**

Plastic pollution and disposal of non-degradable plastic packaging are widespread problems affecting the environment. The development of a fully biodegradable alternative foam packaging with excellent water barrier properties from polysaccharides is quite challenging. In this work, micro-fibrillated cellulose fiber-reinforced-starch foams (MFC-SFs) were crosslinked with two poly(siloxane)-based crosslinking agents to enhance their strength and water barrier properties. The polysiloxane crosslinking agents studied were a cationic

---

\* Corresponding author. Email: [mahbubul.hassan@arts.ac.uk](mailto:mahbubul.hassan@arts.ac.uk) (M. M. Hassan)

† The current address is: Institute of Fashion Textiles and Technology, University of the Arts London, 20 John Prince's Street, London W1G 0BJ, United Kingdom.

trimethylsiloxy-terminated poly(aminoethyl aminopropyl methyl siloxane)-co-poly(dimethylsiloxane) or PAEAPS-co-PDMS, and a non-ionic siloxy-terminated poly(dimethylsiloxane) or TMS-t-PDMS. The applied dosage of polysiloxane crosslinking agents was varied from 1.33 to 5.32% to achieve the optimum strength and moisture barrier properties. The results show that the tensile strength increased from 1.78 MPa for the control to 2.76 MPa for the MFC-SF crosslinked with 5.32% PAEAPS-co-PDMS. The corresponding tensile strength for the MFC-SF crosslinked with TMS-t-PDMS was 2.53 MPa, still considerably higher than the control MFC-SF. The water absorption also decreased from 326.8% for the control to 102.5 and 79.8% for the MFC-SFs crosslinked with 5.32 % PAEAPS-co-PDMS and TMS-t-PDMS respectively. The crosslinking of MFC-SFs with TMS-t-PDMS provided better hydrophobicity compared to the crosslinking with PAEAPS-co-PDMS. The developed packaging could be a promising alternative to non-degradable plastic foam packaging.

*Keywords:* Cellulose fiber-reinforced starch foams; Polysiloxane crosslinking agent; Mechanical and viscoelastic properties

## **1. Introduction**

Plastic foam packaging is extensively used for the packaging of foods including raw meats, fruits and vegetables, fish, and also for other purposes. Many of the plastics used, such as high and low-density polyethylene, polystyrene, poly(ethylene-co-vinyl acetate), polyethylene terephthalate, and polypropylene, are not biodegradable. Very little of the packaging wastes are collected at the kerbside for recycling and most of them often end up discarded in the environment creating plastic pollution. These non-biodegradable plastics not

only cause blockage in urban drainage systems but also are harmful to aquatic and marine animals and fishes. As packaging materials have very low value and are discarded after their use, they need to be very cheap and lightweight as the increase in packaging weight increases the transportation cost of the product. Foam packaging made of expanded polystyrene and polyurethane is popular due to its extremely low density, heat insulation, non-abrasive and excellent cushioning properties that protect the fragile items from impact damage [1-3]. However, the recycling of foam packaging is economically unattractive because of its very low weight per volume and dispersed geographic location at end of life. Polyurethane foam packaging is produced by reacting polyols with diisocyanate. Polyols derived from natural feedstocks are reacted with aliphatic diisocyanates to make fully natural polyurethane. However, polyurethane foams are not biodegradable in anaerobic conditions [4]. The development of packaging made of alternative biodegradable polymers that can reduce carbon footprint, pollution risks, and greenhouse gas emissions is desirable and may resolve the problems associated with expanded polystyrene and polyurethane foam packaging. The application of biomasses and natural polymers has been studied for the development of biodegradable plastics. However, many of these biomasses and natural polymers are highly hydrophilic, which limits their application. They are unsuitable for applications where they will encounter water, such as packaging of fish, meat, and cooked foods, and the storage of the packaged foods in the freezing environment, because the contact and absorption of moisture will affect their dimensional stability. Polysaccharides, such as starch, are water-insoluble, biodegradable, and abundantly available renewable natural polymers, that have been extensively studied for the development of bioplastics. Starch is a carbohydrate polymer containing amylose with a linear structure of  $\alpha$ -1,4 linked glucose units, and amylopectin with a highly branched structure of short  $\alpha$ -1,4 chains linked by  $\alpha$ -1,6 bonds [5]. Gelatinous starch can be processed like thermoplastic polymers and therefore has attracted the attention

of innovators for the development of bioplastics. However, starch-made foam packaging is weak and therefore needs to be reinforced. Cornstalk fibers [6], talc [7], sesame cake [8], grape stalks [9], micro-fibrillated cellulosic [10,11], malt bagasse [12], and also some nanofillers, such as clays and cellulose nanofibers [13], have been studied to increase the strength of the starch films and foam packaging.

Starch has abundant hydrophilic hydroxyl groups, and therefore starch-made foams easily absorb moisture. Several methods, such as the addition of polylactic acid (PLA) and polycaprolactone (PCL), coatings with PLA, and chemical crosslinking have been investigated to enhance their water barrier properties with limited success [14-18]. There is hardly any benefit in the addition of a small percentage of PLA to starch as it is insufficient to change the starch foam's hydrophilic behavior. In the case of coating with hydrophobic polymers, if a small hole is formed in the hydrophobic coating, the water barrier properties and dimensional stability will be compromised. The blocking of hydroxyl groups by crosslinking is envisaged as a solution. Several crosslinking agents, such as citric acid [6,10], glutaraldehyde [19,20], sodium hexametaphosphate (SHMP) [21], and glyoxal [22], have been studied with some level of success. Of them, glutaraldehyde and glyoxal are toxic, and therefore are unsuitable for the crosslinking of food packaging. The SHMP crosslinking provided only marginal improvement in hydrophobicity of the produced foam packaging as the contact angle was only  $66^\circ$  [16]. Comparatively, citric acid crosslinking provided better hydrophobicity as the contact angle of the crosslinked starch/cellulose composite foam increased to  $102.1^\circ$  for the 5% citric acid (wt/wt) but the rigidity of the foam increased considerably making the packaging brittle.

Siloxanes constitute a group of low molecular weight compounds, organosilicon oligomers, and polymers, which play a very important role in human life. They are used in various human applications, such as prosthetics, medical implants, biomedical devices, and

other applications [23-25], but apparently never studied for the crosslinking of starch foams. It is envisaged that the crosslinking of starch/cellulose composite foams with polymeric siloxane crosslinking agents will block some of the hydroxyl groups of cellulose and starch reducing the hydrophilicity of the foam packaging. In this work, starch-cellulose composite foams were crosslinked with amino and hydroxy-functional polysiloxane polymers to enhance the strength and water barrier properties of starch foams. Starch foams are quite weak and therefore micro-fibrillated cellulose was added to reinforce the starch foam packaging. To the best of our knowledge, no published article has reported crosslinking of thermoplastic starch or cellulose reinforced starch composite foam crosslinked with polysiloxane-based crosslinking agents.

## **2. Experimental section**

### *2.1. Materials*

Potato starch with an average granule size of 95  $\mu\text{m}$  containing 29.3 % amylose and 70.7 % amylopectin and carnauba wax were purchased locally. Microfibrillated cellulose powder derived from wood pulp with a length between 500 to 800  $\mu\text{m}$  and a width between 15 to 34  $\mu\text{m}$ , was supplied by Innventia AB (Stockholm, Sweden). Lutensol TO 12 (C13-fatty alcohol ethoxylate), anionic surfactant, was supplied by BASF Chemicals, Germany. The trimethylsilyl-terminated copolymer of poly(N-(2-aminoethyl)-3-aminopropylmethyl siloxane)-co-poly(dimethylsiloxane) or PAEAPS-co-PDMS, and trimethoxysilyl-terminated poly(dimethylsiloxane) or TMS-t-PDMS were supplied by BASF Chemicals (Germany) and Clariant Chemicals (Switzerland) respectively. The chemical structures of PAEAPS-co-

PDMS and TMS-t-PDMS are shown in Fig. S1 (Supplementary Material). Isotridecanol ethoxylate, a non-ionic emulsifier was supplied by Merck (Germany).

## *2.2. Preparation of polymer emulsions*

The required quantity of isotridecanol ethoxylate was mixed with 38 g PAEAPS-co-PDMS in a glass beaker by slow magnetic stirring. Then 5 ml water was slowly added to it with stirring. Then the speed of stirring increased and another 10 mL of water was added to it. Then another 45 ml water was added to it and stirring continued for 60 min and the pH was adjusted to 5. Similarly, TMS-t-PDMS emulsion was prepared using the same procedure but Lutensol TO 12 was used as an emulsifier as suggested by the manufacturer of TMS-t-PDMS.

## *2.3. Characterization of siloxane polymers*

The infrared (IR) spectra of the purified siloxane copolymers were recorded using a Nicolet FTIR (Model: Summit Pro, Thermo Fisher Scientific Corp., USA) equipped with an attenuated total reflectance (ATR) attachment using a diamond crystal. 64 scans were carried out and the average is reported. The micellar size of the polysiloxane emulsions was measured by multiangle dynamic light scattering (Model: Zetasizer Ultra, Malvern Panalytical Ltd., Malvern, UK).

#### 2.4. Preparation of crosslinked MFC-SFs

The rectangular-shaped MFC-SF samples were fabricated by one-step compression molding. The chemical composition of the MFC-SF sheet-making mixture is shown in Table 1. The required amount of starch, cellulose powder and carnauba wax was mixed using a domestic food blender. The required quantity of PAEAPS-co-PDMS or TMS-t-PDMS crosslinking agent mixed with water was added slowly to the starch mixture with the blender running at 30 rpm and after the addition of all water, the speed of the blender was increased to 200 rpm to make a homogenized mixture of starch, cellulose, Carnauba wax, and the crosslinking agent.

**Table 1.**

The dough compositions used for the fabrication of starch/cellulose/PLA foam composites

Sample ID.	Dry weight (%)					
	Starch	Cellulose	PAEAPS-co-PDMS	TMS-t-PDMS	Carnauba wax	Water
Control	44.41	15.16	-	-	1.86	40.43
PAEAPS-co-PDMS	44.41	15.16	1.33	-	1.86	39.10
PAEAPS-co-PDMS	44.41	15.16	2.66	-	1.86	37.77
PAEAPS-co-PDMS	44.41	15.16	5.32	-	1.86	35.11
TMS-t-PDMS	44.41	15.16	-	1.33	1.86	39.10
TMS-t-PDMS	44.41	15.16	-	2.66	1.86	37.77
TMS-t-PDMS	44.41	15.16	-	5.32	1.86	35.11

For the control sample, no crosslinker but only water was added to the starch mixture. The final moistened mixture was mixed at 200 rpm for 90 s. A predetermined amount of the moistened starch mixture was placed in a rectangular-shaped mold and 2.30 mm thick

composite foam sheets were prepared by compression molding at 2 MPa pressure at 220 °C for 120 s. Of the hydroxyl groups in starch and cellulose, the OH group at position C6 is the most reactive because of its lower steric hindrance compared to other OH groups at C2 and C3 positions [26], and therefore crosslinking takes place predominantly between OH groups at the C6 position of various molecular chains of starch and cellulose. The reactive polysiloxane crosslinking agents not only reacted with OH groups of starch and cellulose macromolecular chains but also self-crosslinked as shown in Fig. 1. The prepared MFC-SF samples were stored at  $20 \pm 2$  °C and  $65 \pm 2$  % relative humidity until various characterizations were carried out.

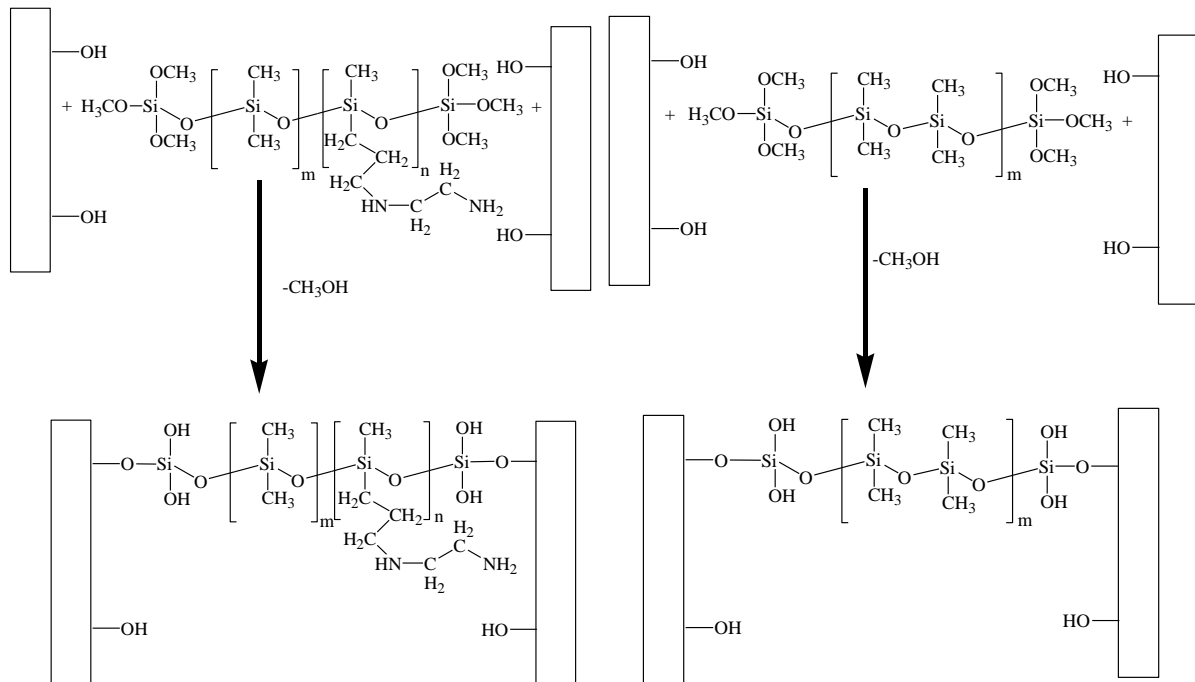


**Fig. 1.** Mechanisms of crosslinking of cellulose and starch with PAEAPS-co-PDMS (left) and TMS-t-PDMS (right).

## 2.5. Measurement of physicochemical properties

The density of the neat MFC-SF and MFC-SFs crosslinked with various concentrations of PAEAPS-co-PDMS and TMS-t-PDMS was measured by using the following equations:

$$\rho = \frac{m}{v} \quad [1]$$

where,  $\rho$  = density,  $m$  = mass of the foam and  $v$  = volume of the foam. 10 samples were tested for each foam and the averages are reported here. Thermo-gravimetric analysis (TGA) of the foam composites crosslinked with various weight% of reactive polysiloxane crosslinkers were carried out from room temperature to 500 °C at a heating rate of 5 °C/min by using a thermogravimetric analyzer (Model 550, TA Instruments Inc., New Castle, USA) under nitrogen atmosphere. At least three samples were tested, and the specimen TGA curves were shown.

The contact angle was measured in dynamic mode by using a KSV CAM 100 Contact Angle Measurement Apparatus (KSV Instruments, Finland). The contact angles were quantified by using the Young-Laplace equation using the software supplied with the apparatus. The first measurement was taken immediately after placing the water droplet and the successive measurements were taken at 120 s intervals until 480 s. For each sample, the contact angle was measured at 10 places on both sides of the samples, and the average contact angle is reported here. The moisture content of the control cellulose reinforced starch foam and starchfoams crosslinked with two polysiloxane crosslinking agents was measured at 20±2 °C and 65±2% relative humidity. The samples were conditioned for 48 h before testing and then weighed. Then the oven-dry weight was measured after drying to the constant weight at 105±2 °C by Kern Rapid Drying Instrument.

## 2.6. Mechanical properties

The effect of increasing the concentration of PAEAPS-co-PDMS and TMS-t-PDMS on the tensile and flexural properties of the MFC-SFs was studied. Dog-bone shaped specimens of  $15.0 \times 70$  mm in dimension crosslinked with various weight% of PAEAPS-co-PDMS and TMS-t-PDMS were cut from the rectangular-shaped compression-molded MFC-SF samples and preconditioned at least 48 h at  $20 \pm 2$  °C and  $65 \pm 2$  % relative humidity [15]. The tensile properties were measured at that conditions by an Instron Universal Tensile Testing (Model 4204, Instron Inc., USA) at a crosshead speed of 20 mm/min and a gauge length of 30 mm. Flexural tests were carried out according to ASTM Test Method D 790-03 using a 3-point flexural test rig attached to an Instron Universal Tensile Testing machine at a crosshead speed of 10 mm/min using a span length of 40.0 mm at the same atmospheric conditions the tensile measurements were carried out. For the flexural measurements, the sample size was  $60 \times 20 \times 2.3$  mm, and samples were preconditioned at the standard atmospheric conditions for 48 h before testing. In this method, the test specimens were supported at both ends, and force was applied from the top in the middle of the specimen. From the force-displacement curve, the flexural strength and flexural modulus were calculated. The vertical displacement was measured at the center of the span using an LVDT displacement transducer. The flexural strength and flexural modulus were calculated according to the following formulae:

$$\text{Flexural strength } (\sigma) = \frac{3FL}{2bh^2} \quad [2]$$

$$\text{Flexural or bending modulus } (E_{bend}) = \frac{L^3 \times F}{4bh^3d} \quad [3]$$

where, L = span length, F = force, b = sample width, h = sample thickness and d = deflection.

For each sample, at least 10 tests were carried out and the averages are reported here.

### *2.7. Dynamic mechanical thermal analysis*

For the dynamic mechanical thermal analysis (DMTA), PAEAPS-co-PDMS and TMS-t-PDMS crosslinked samples of  $15 \times 56 \times 2.2$  mm size were cut and stored at standard atmospheric conditions before carrying out the analysis. The DMTA analysis was carried out in 3-point flexural mode using a dynamic thermal mechanical analyzer (Model RSA-G2, TA Instruments, New Castle, USA). The dynamic measurements were recorded during a heat ramp starting from  $T = 25$  °C to  $150$  °C at a rate of  $5$  °C/min and a frequency of  $1$  Hz and  $0.1$  % strain. The storage modulus ( $E'$ ), loss modulus ( $E''$ ), and loss factor ( $\tan \delta$ ) of the samples were measured in triplicate and examples of a typical curve are presented.

### *2.8. Surface and morphological characteristics*

The neat and the cracked surface of composite foams were characterized by scanning the surface without any conductive coating using backscattered mode on a Hitachi scanning electron microscope (Model: TM3030Plus, Hitachi Corporation, Japan) at an accelerating voltage of  $15$  kV.

The infrared (IR) spectra of the composite foam surfaces were recorded using a Nicolet FTIR (Model: Summit Pro, Thermo Fisher Scientific Corp., USA) equipped with an attenuated total reflectance (ATR) attachment using a diamond crystal from  $450$  to  $3600$   $\text{cm}^{-1}$ . The samples were placed flat on the upper side of the crystal. Good fiber to crystal contact

was ensured by applying a 50 N force using a calibrated torque wrench. 64 scans were carried out for each sample.

## 2.9. Statistical analysis

All tests were performed at least 10 times except otherwise stated. SPSS (v. 20) statistical software was used to perform analysis of variance (ANOVA) to test the statistical significance of results achieved in this work. Bonferroni post hoc multiple-range test was performed, and pair-wise comparison was made between control MFC-SFs and MFC-SFs crosslinked with various concentrations of polysiloxane crosslinking agents, and also between MFC-SFs crosslinked with different concentrations of polysiloxane crosslinking agents. A  $p$ -value  $< 0.05$  was considered statistically significant [27].

## 3. Results and discussion

### 3.1. FTIR characterization of reactive polysiloxane crosslinking agents

The chemical structure of the reactive polysiloxane crosslinking agents was characterized by FTIR and the micelle size of the two emulsions was assessed by dynamic light scattering. Fig. 2 shows the ATR-FTIR spectra of control and crosslinked MFC-SFs. The spectrum of PAEAPS-co-PDMS shows characteristic IR bands of PDMS at 785, 1008, 1081, 1258, and 1415  $\text{cm}^{-1}$ . They are due to the  $-\text{CH}_3$  rocking and Si-C stretching in Si- $\text{CH}_3$  ( $786 \text{ cm}^{-1}$ ), Si-O-

Si ( $1008$  and  $1081\text{ cm}^{-1}$ ),  $\text{CH}_3$  deformation in Si- $\text{CH}_3$  ( $1258\text{ cm}^{-1}$ ), C-C ( $1415\text{ cm}^{-1}$ ). Compared to the spectrum of PDMS, the spectrum also shows extra IR bands at  $2850$ ,  $2966$ , and  $3410\text{ cm}^{-1}$  extra, and they are associated with symmetric C-H stretching ( $2850\text{ cm}^{-1}$ ), asymmetric  $\text{CH}_3$  stretching ( $2963\text{ cm}^{-1}$ ) of siloxy groups ( $3410\text{ cm}^{-1}$ ). It shows also extra IR bands at  $1560$ ,  $1650$ , and  $1710\text{ cm}^{-1}$  due to the amide II band and the N-H stretching of amine II;  $\text{CONH}_2$  group suggesting the successful formation of amino-functional PDMS. In particular, the amide I band at  $1655\text{ cm}^{-1}$  or the amide II band at  $1560\text{ cm}^{-1}$  is identified as characteristic N-acetylation bands associated with amine and amide groups [28]. On the other hand, the spectrum of TMS-t-PDMS does not show any IR bands at  $1560$ ,  $1650$ , and  $1710\text{ cm}^{-1}$  and also the intensity of the siloxy band at  $3410\text{ cm}^{-1}$  is considerably lower compared to the siloxy band intensity observed for the PAEAPS-co-PDMS suggesting the decreased number of siloxy groups are present in the TMS-t-PDMS polymer.

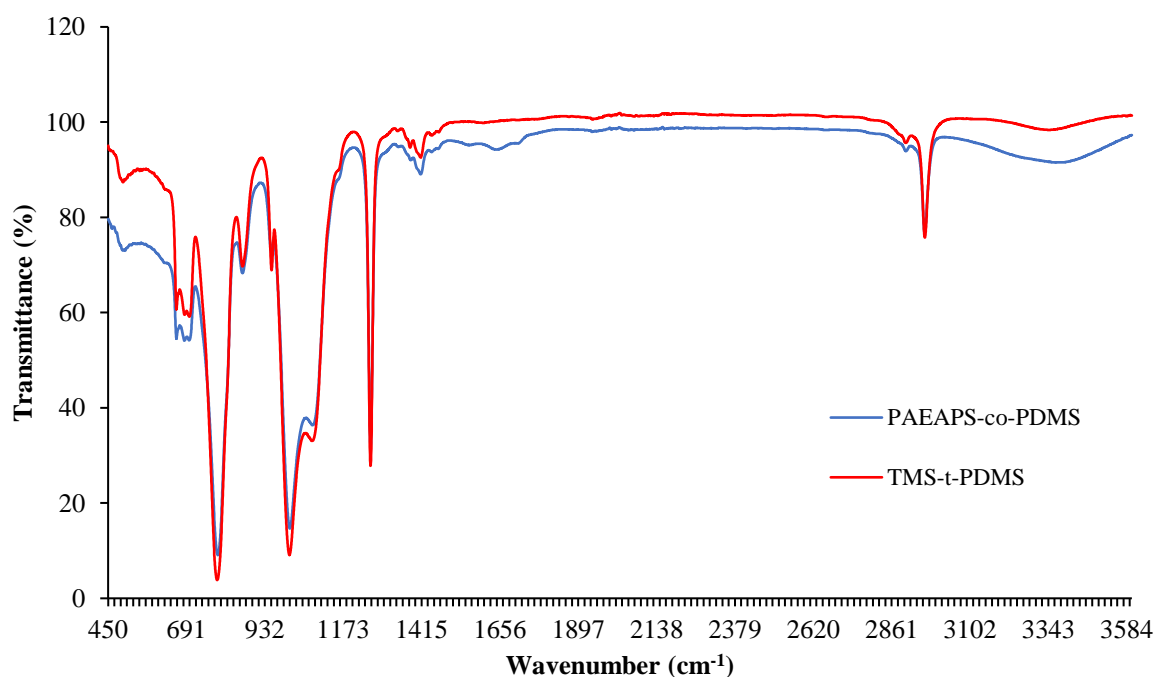


**Fig. 2.** FTIR spectra of reactive polysiloxane crosslinkers, PAEAPS-co-PDMS, and TMS-t-PDMS.

The intensity vs the micellar size curves of the triplicate samples of PAEAPS-co-PDMS (top) and TMS-t-PDMS emulsions are shown in Fig. S2 (Supplementary Material). It can be seen that for each type of emulsion, the triplicate samples showed the same micellar size, but their intensity only slightly varied. The micellar size of the PAEAPS-co-PDMS and TMS-t-PDMS polymers were  $39.48 \pm 0.13$  and  $77.21 \pm 0.16$  nm respectively. It is evident that both polymers formed nano-emulsions but the micellar size of the TMS-t-PDMS emulsion was almost double of the PAEAPS-co-PDMS emulsions. Both the formed emulsions were very stable and little change in micellar size was observed even after six months.

### *3.2. Rheological properties*

The effect on the stiffness and viscoelastic properties of MFC-SFs generated by crosslinking with two silicone polymeric crosslinking agents was assessed by dynamic mechanical thermal analysis. Fig. 3 (top) shows the representative storage moduli ( $E'$ ) curves of MFC-SFs crosslinked with 1.33, 2.66, and 5.32% (wt/wt) PAEAPS-co-PDMS and TMS-t-PDMS from room temperature to 150 °C. Silicone polymers are elastomeric polymers and therefore their crosslinking with starch and MFC caused a decrease in stiffness of the produced foam sheets instead of increasing the stiffness as observed for the citric acid crosslinking of the similar starch foams [15]. The storage modulus ( $E'$ ) of the starch foams decreased with an increase in the concentration of both crosslinking agents. For both polymeric silicone crosslinking agents, the storage modulus of the starch foams decreased

with an increase in the temperature suggesting a progressive reduction of stiffness with the increased temperature. In the case of TMS-t-PDMS, the control MFC-SF showed higher stiffness than all polysiloxane crosslinked foams from room temperature to 45 °C but after which the storage modulus was similar to storage modulus exhibited by the MFC-SFs crosslinked with TMS-t-PDMS up to 2.66% (wt/wt). The starch foam crosslinked with 1.33% TMS-t-PDMS showed slightly better stiffness from 60 to 70 °C compared to the control starch foam. For both types of polymeric crosslinking agents, the composite foam crosslinked with 5.32% (w/w) TMS-t-PDMS showed the lowest storage modulus ( $E'$ ). At 30 °C, the storage modulus of the control MFC-SF was  $8.13 \times 10^8$  Pa, which decreased to  $7.68 \times 10^8$  Pa for the MFC-SF crosslinked with 1.33% PAEAPS-co-PDMS. The increase in the weight% of PAEAPS-co-PDMS to 2.66% and 5.32% decreased the storage modulus ( $E'$ ) to  $0.654 \times 10^8$  Pa and  $5.63 \times 10^8$  Pa respectively. On the other hand, in the case of TMS-t-PDMS, at 30 °C the storage modulus decreased to  $7.67 \times 10^8$  Pa for the 1.33% TMS-t-PDMS. The further increase in the TMS-t-PDMS weight% to 2.66 and 5.32% further decreased to  $6.53 \times 10^8$  Pa and  $5.65 \times 10^8$  Pa respectively. However, with an increase in temperature the storage modulus slowly decreased but the greatest effect was observed from room temperature to 50 °C when the highest decrease in the storage modulus or stiffness was observed. With the increase in temperature to 100 °C, the storage modulus of the control samples decreased to  $6.12 \times 10^8$  Pa but for the MFC-SFs crosslinked with 1.33, 2.66, and 5.32% PAEAPS-co-PDMS, the storage modulus decreased to  $6.21 \times 10^8$ ,  $6.14 \times 10^8$ ,  $5.3 \times 10^8$  Pa respectively. The corresponding storage modulus values for the MFC-SFs crosslinked with TMS-t-PDMS were  $6.10 \times 10^8$ ,  $5.15 \times 10^8$  Pa, and  $4.44 \times 10^8$  Pa respectively.

The loss modulus ( $E''$ ) data also showed a trend similar to the storage modulus data, i.e. the loss modulus of the composite foam decreased with an increase in the weight% of PAEAPS-co-PDMS and TMS-t-PDMS as shown in Fig. 3 (bottom). The non-crosslinked

starch cellulose composite showed the highest loss modulus and the composite foam crosslinked with 5.32% (w/w) TMS-t-PDMS showed the lowest loss modulus. Similar to the storage modulus, the loss modulus also decreased with an increase in temperature.

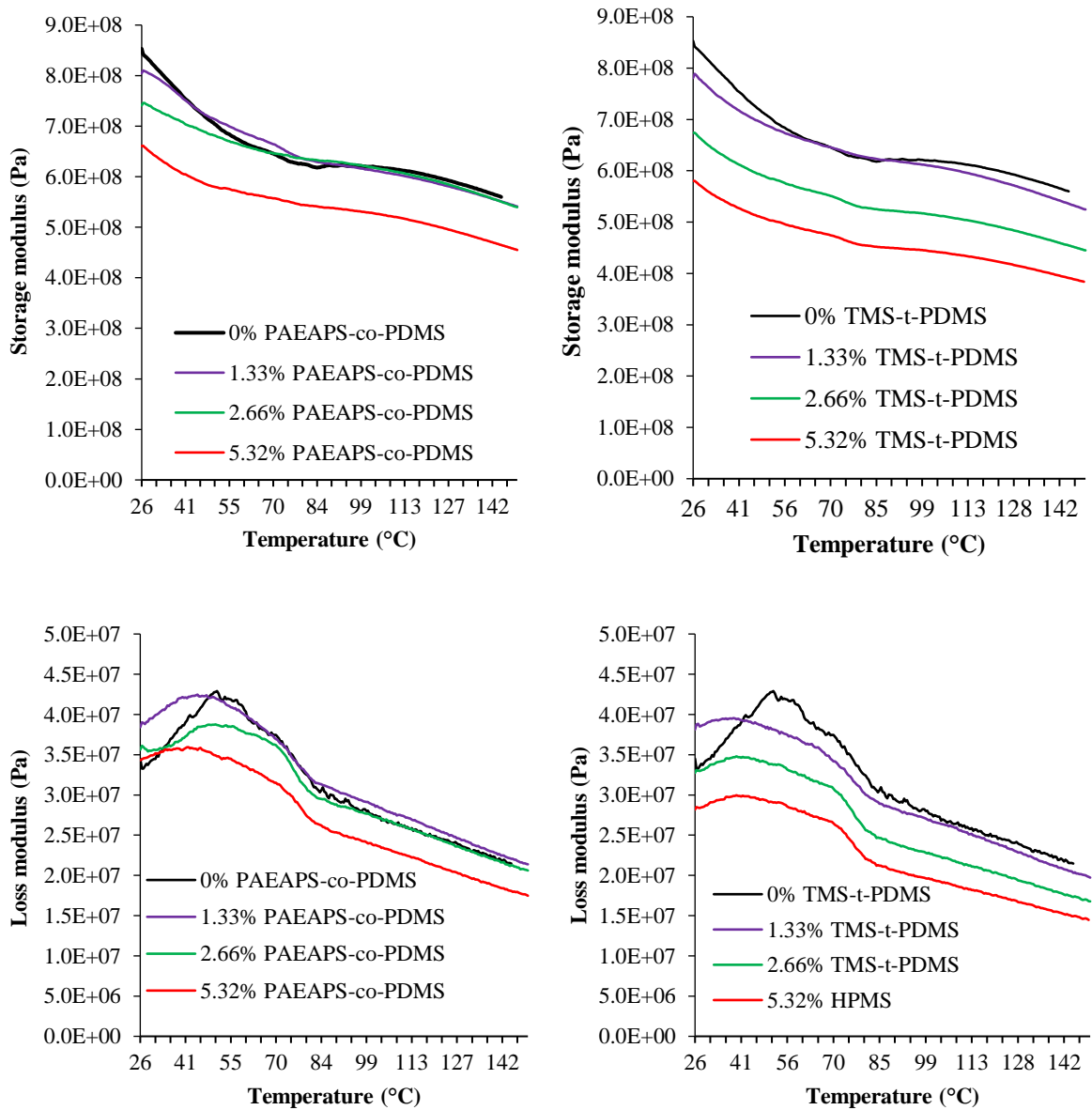


**Fig. 3.** Effect of temperature on storage (top) and loss (bottom) moduli of MFC-SFs crosslinked with different concentrations of PAEAPS-co-PDMS (left) and TMS-t-PDMS (right).

Tan  $\delta$  is the ratio between the storage modulus and loss modulus which represents mechanical damping or internal friction in a viscoelastic system. The higher the value of Tan  $\delta$ , the higher the viscosity of that material. The effect of crosslinking with PAEAPS-co-PDMS on the mechanical loss factor, Tan  $\delta$ , of the MFC-SFs is shown in Fig. S3 (Supplementary Materials) from room temperature to 150 °C. Neither the control and PAEAPS-co-PDMS crosslinked MFC-SFs show any sharp Tan  $\delta$  peak, rather all of them show a broad peak around 55 °C indicating that none of the foams material show phase transition from glass to rubber, i.e. none of them show any precise glass transition temperature ( $T_g$ ). However, in the case of 1.33% PAEAPS-co-PDMS, the peak height was smaller compared to the control foam until 84 °C but over that temperature, no effect was observed for the PAEAPS-co-PDMS at all concentrations. The starch foams crosslinked with TMS-t-PDMS also showed similar behavior.

### *3.3. Density, and tensile and flexural properties*

The effect of the increase of weight% of PAEAPS-co-PDMS and TMS-t-PDMS on the density of the MFC-SFs is shown in Table 1. The control MFC-SF had a density of 0.3412 g/cm<sup>3</sup> but the crosslinked foam showed a slightly higher density than the control MFC-SF. The density of the foam increased with an increase in the weight% of the crosslinking agent and the MFC-SFs crosslinked with TMS-t-PDMS exhibited slightly higher density compared to the MFC-SFs crosslinked with PAEAPS-co-PDMS. The density of the MFC-SFs increased from 0.3493 to 0.3644 g/cm<sup>3</sup> when the weight% of PAEAPS-co-PDMS was increased from

1.33% to 5.32%. The corresponding values for the MFC-SFs crosslinked with TMS-t-PDMS were 0.3588 and 0.3723 g/cm<sup>3</sup> respectively.

Packaging materials should have a minimum strength for their application. Table 2 shows the mechanical properties of MFC-SFs crosslinked with PAEAPS-co-PDMS and TMS-t-PDMS. The tensile strength of MFC-SFs considerably increased with the crosslinking with reactive polysiloxane crosslinking agents. Of them, PAEAPS-co-PDMS provided slightly

**Table 2.**

Density and mechanical properties of MFC-SFs crosslinked with polysiloxane crosslinking agents.

Sample ID	Density (g/cm <sup>3</sup> )	Tensile strength (MPa)	Breaking force (MPa)	Elongation at break (%)
Control	0.3412	1.78 (0.05)	1.71(0.05)	2.05 (0.28)
1.33% PAEAPS-co-PDMS	0.3493	2.45 (0.07)*	2.11 (0.04)*	8.05 (0.41)*
2.66% PAEAPS-co-PDMS	0.3538	2.63 (0.06)*	2.55 (0.07)*	8.63 (0.48)
5.32% PAEAPS-co-PDMS	0.3644	2.76 (0.06)*	2.65 (0.04)*	8.48 (0.51)
1.33% TMS-t-PDMS	0.3588	2.26 (0.09)*	1.82 (0.05)*	9.88 (0.97)*
2.66% TMS-t-PDMS	0.3683	2.41 (0.07)*	2.10 (0.07)*	6.12 (0.81)*
5.32% TMS-t-PDMS	0.3723	2.53 (0.09)*	2.20 (0.06)*	5.82 (0.32)

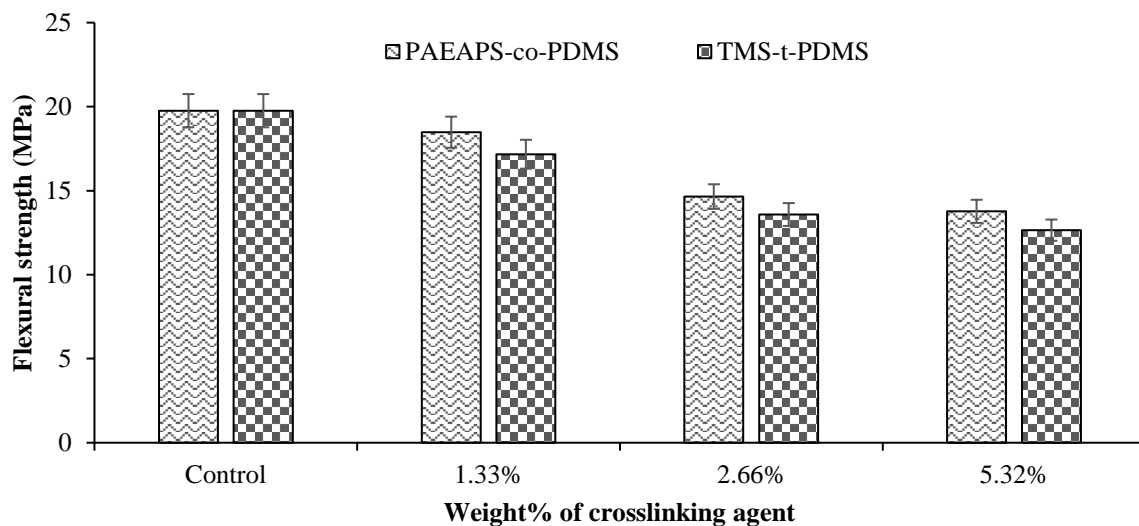
\**p*-value less than 0.05

better tensile strength compared to the TMS-t-PDMS. Even at 1.33% (wt/wt) applied dosage, the tensile strength substantially increased. The control MFC-SFs exhibited poor tensile strength (1.78±0.85 MPa) and elongation (1.95%), which increased to 2.45±0.36 MPa and

7.62% respectively for the foam crosslinked with 1.33% (wt/wt) PAEAPS-co-PDMS. The tensile strength increased from  $2.45 \pm 0.36$  MPa to  $2.76 \pm 0.35$  MPa when the concentration of PAEAPS-co-PDMS increased from 1.33 to 5.32% (wt/wt). The other crosslinking agent, TMS-t-PDMS, also showed similar behavior but showed a slightly lower increase in tensile strength. On the other hand, the elongation of the foams increased with an increase in the crosslinking agent concentrations up to 2.66% (wt/wt) but after which the elongation at peak slightly decreased. The chemical crosslinking is known to increase the tensile strength but decreases the elongation. However, the polymeric crosslinking agents used in this work are elastomers, and therefore instead of decreasing, the elongation increased with an increase in the crosslinking agent dosage.

The MFC-SFs are quite rigid and therefore they are susceptible to impact damage. Therefore, it is necessary to evaluate their flexural strength to reduce their possible impact damage. The flexural strength of the MFC-SFs decreased with an increase in the concentration of polysiloxane crosslinking agents. With the addition of 1.33% (wt/wt) PAEAPS-co-PDMS, the flexural strength decreased only marginally (18.5 MPa) but with a further increase in the concentration of PAEAPS-co-PDMS to 5.32% (wt/wt), the flexural strength decreased to 13.8 MPa. The MFC-SFs crosslinked with TMS-t-PDMS also exhibited similar behavior but decreased the rigidity higher than the rigidity observed for the PAEAPS-co-PDMS crosslinked MFC-SFs. Trimethylsiloxy-terminated PDMS are usually widely used as a plasticizer in silicone adhesives, and they are known to create a networked structure [29]. Therefore, although chemical crosslinking is reported to increase the rigidity of the starch/cellulose composite foam [10], as PDMS is a rubbery polymer, the addition of it to cellulose reinforced starch foams should reduce their bending rigidity. The flexural strength exhibited by the MFC-SFs crosslinked with polysiloxane crosslinking agents is consistent with the storage modulus of the crosslinked MFC-SFs measured by the DMTA.

Fig. 4 (bottom) shows the flexural modulus of the MFC-SFs crosslinked with PAEAPS-co-PDMS and TMS-t-PDMS. The control MFC-SF sample exhibited the highest flexural modulus (323.1 MPa), but when they were crosslinked with 1.33% (wt/wt) PAEAPS-co-PDMS, the flexural modulus dropped to 269.7 but with a further increase in the concentration of PAEAPS-co-PDMS the flexural modulus increased with an increase in the concentration of the crosslinking agent. For the 5.32% (wt/wt) PAEAPS-co-PDMS, the flexural modulus increased to 324.2 MPa, almost similar to the flexural modulus of the control MFC-SF. The TMS-t-PDMS crosslinked MFC-SFs also showed similar behavior but slightly lower flexural modulus compared to the flexural modulus exhibited by the PAEAPS-co-PDMS crosslinked MFC-SFs.



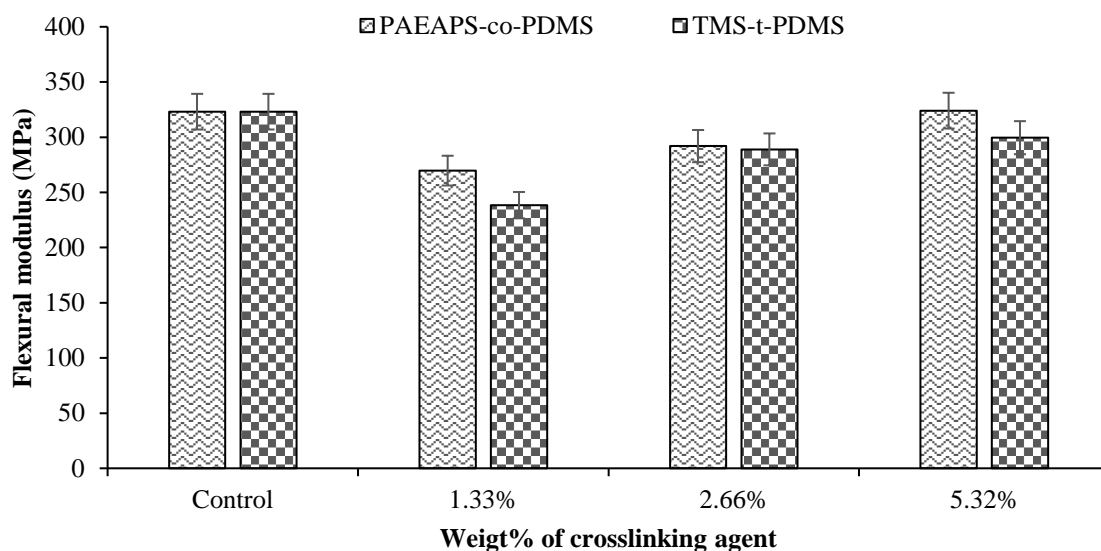
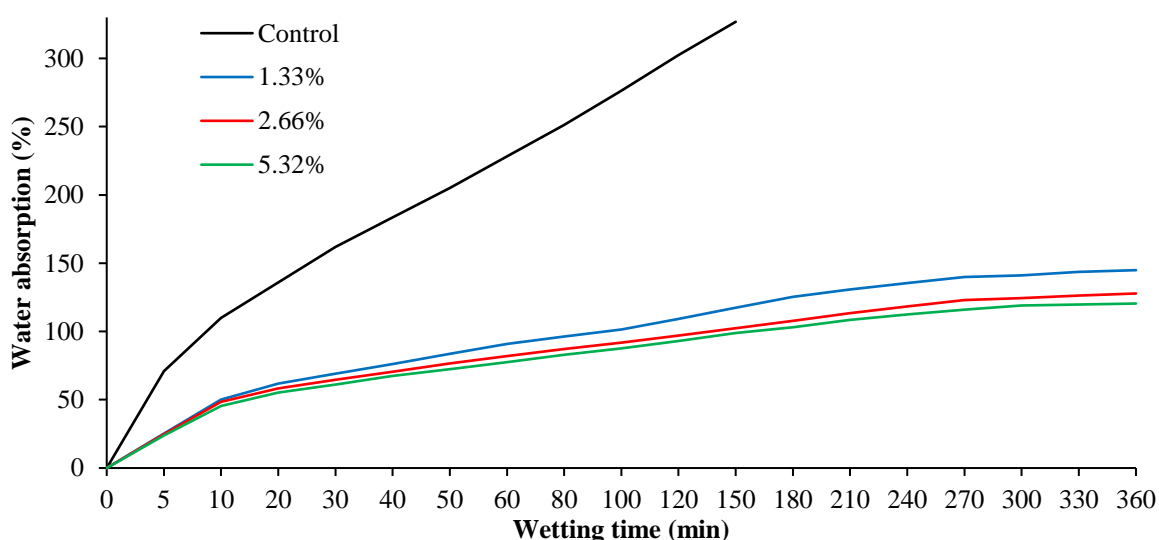


**Fig. 4.** Flexural strength (top) and flexural moduli of MFC-SFs crosslinked with various concentrations of PAEAPS-co-PDMS and TMS-t-PDMS crosslinking agents.

### 3.4. Effect of crosslinking on moisture and water absorption

The effect of polysiloxane crosslinking with cellulose and starch on the moisture content of the formed MFC-SFs was assessed to observe whether the moisture absorption by the starch foams is affected by crosslinking. As expected, the control MFC-SF showed moderately high moisture content (12.3%), but with 1.33% (wt/wt) PAEAPS-co-PDMS and TMS-t-PDMS, the moisture content reduced to 11.1 and 10.8% respectively (Fig.S4 in Supplementary Material). The moisture content decreased with an increase in the weight% of the crosslinking agents. The moisture content decreased to 10.1 and 9.9% respectively when the weight% of PAEAPS-co-PDMS and TMS-t-PDMS was increased to 5.32% (wt/wt). The TMS-t-PDMS crosslinked MFC-SFs exhibited slightly lower moisture content compared to the MFC-SFs crosslinked with PAEAPS-co-PDMS.

The foam packaging, especially the biobased one, needs to have good water barrier properties. MFC-SF is quite hydrophilic as cellulose and starch both have many hydrophilic hydroxyl groups making them highly water absorbent. Fig. 5 shows the water absorbency of MFC-SFs crosslinked with various concentrations of PAEAPS-co-PDMS and TMS-t-PDMS crosslinking agents. It is evident that crosslinking substantially decreased the water absorbency of the MFC-SFs, i.e. considerably enhanced their water barrier properties. For both crosslinked and non-crosslinked MFC-SFs, the highest water absorption was within 10 min of wetting time, after which the water absorption by the MFC-SFs slowly increased up to 240 min and then reached a plateau. The control SFC-MF was highly hygroscopic and after 150 min, the water absorption increased to almost 327% and the sample disintegrated in water not allowing further water absorbency measurement. On the other hand, the MFC-SFs crosslinked with polysiloxane crosslinking agents exhibited considerably decreased water absorption and the water absorbency decreased with an increase in the crosslinking agent concentration. For the 1.33% (wt/wt) PAEAPS-co-PDMS, the water absorbency at 150 min was only 117% compared to 327% for the control, which reached 145% after 360 min of



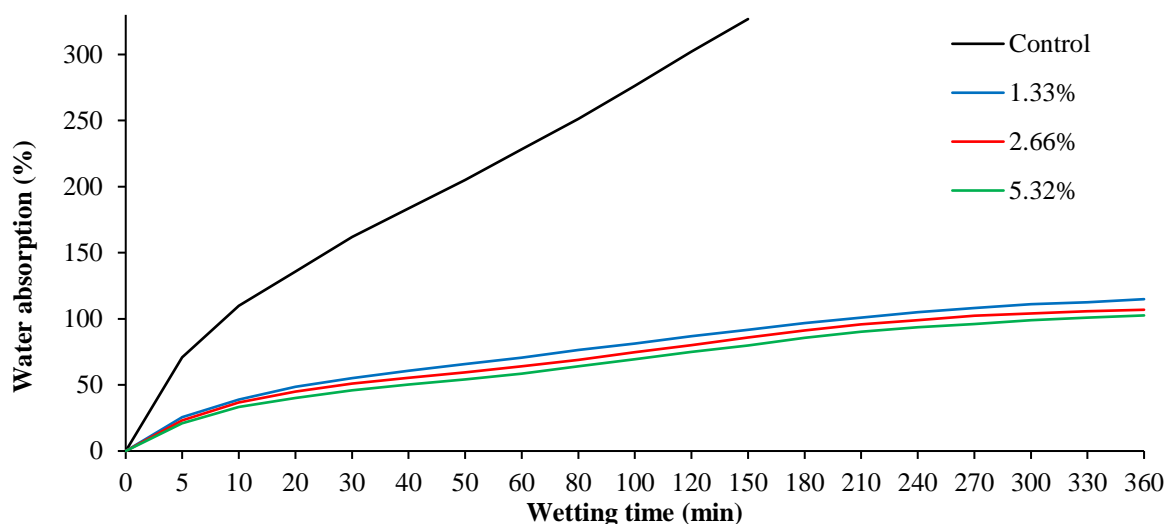


**Fig. 5.** Effect of wetting time on the water absorption by MFC-SFS crosslinked with various concentrations of PAEAPS-co-PDMS (top) and TMS-t-PDMS (bottom).

soaking. The sample did not disintegrate and was fully intact even after 360 min soaking suggesting extensive crosslinking occurred between cellulose and starch. For the 5.32% (wt/wt) PAEAPS-co-PDMS, the water absorption increased to 120% only at 360 min soaking, almost one-third of the water absorbency exhibited by the control MFC-SF at 150 min of soaking. The MFC-SFs crosslinked with TMS-t-PDMS exhibited considerably better water barrier properties as the water absorption was much lower compared to the MFC-SFs crosslinked with PAEAPS-co-PDMS. In the case of MFC-SFs crosslinked with 1.33 and 5.32% (wt/wt) TMS-t-PDMS, the water absorption decreased to approximately 107 and 102% respectively at 360 min soaking. Compared to the PAEAPS-co-PDMS, the TMS-t-PDMS do not have any water-loving amino groups and therefore provide better hydrophobicity. The polysiloxane crosslinked MFC-SFs exhibited considerably lower water absorption compared to the PLA-containing or citric acid crosslinked MFC-SFs reported earlier [10,15].

### 3.4. Thermogravimetric analysis

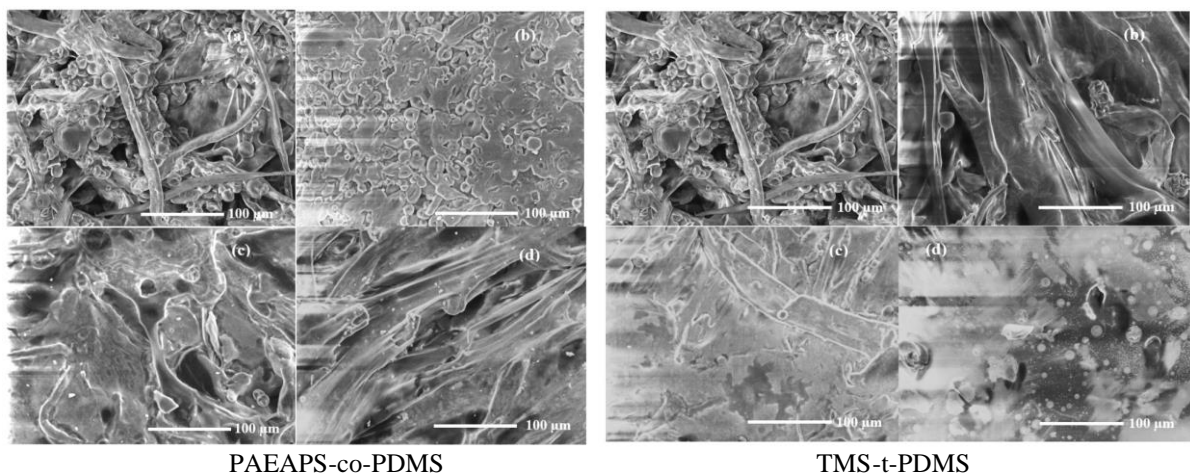
The MFC-SFs need to have good thermal stability as such a type of packaging is used for hot foods. Thermogravimetric analysis was utilized to assess the thermal stability of the control and polysiloxane crosslinked MFC-SFs. The thermal stability of the MFC-SFs improved to a level after crosslinking with polysiloxane-based crosslinking agents, which increased with an increase in the crosslinking agent concentration. as shown in Fig. S5 (Supplementary Material).

The control and the MFC-SFs crosslinked with two polysiloxane-based crosslinking agents, all showed a four-stage weight loss. The weight loss at the first stage from room temperature to 120 °C occurred mainly due to the loss of absorbed moisture by starch and cellulose as both the polymers are hydrophilic [30]. The weight loss that occurred at this stage was quite low, which was approximately 6.1, 6.4, and 5.6% for the control, 2.66% PAEAPS-co-PDMS, and 2.66% TMS-t-PDMS, respectively. Very little weight loss was observed from 120 to 260 °C. For all the MFC-SFs, the most rapid and the highest weight loss occurred at the second stage. For the control foam, the highest weight loss (approx. 54.7%) occurred at 259 to 330 °C due to the degradation of cellulose and starch producing various volatiles including carbon dioxide and carbon monoxide [31]. In the case of MFC-SFs crosslinked with 2.66% (wt/wt) PAEAPS-co-PDMS and TMS-t-PDMS, the weight loss took place between 278 to 330 °C was 52 and 49%, respectively, much lower compared to the weight loss occurred for the control MFC-SF at that temperature. The second highest weight loss occurred at the 3<sup>rd</sup> stage due to further degradation of the degraded components of starch and cellulose and the crosslinking agent. The weight loss that occurred for the

control MFC-SF from 330 to 360 °C was another 18.1%. However, for the 2.66% PAEAPS-co-PDMS and TMS-t-PDMS, the corresponding values were and 17.2 and 19.6%, respectively. The ash content at 600 °C in the case of control MFC was only 12.3% but for the 2.66% PAEAPS-co-PDMS and TMS-t-PDMS, the corresponding values were 13.1 and 13.8% respectively.

### 3.5. Morphologies of crosslinked MFC-SFs

The neat surface of control MFC and also MFC-SFs crosslinked with 1.33., 2.66, and 5.32% (wt/wt) are shown in Fig. 6. It can be seen that the surface of the control MFC-SF was quite uneven with large groves and also MFCs are loosely bonded to the surface. Some non-gelatinized starch particles are also clearly visible on the surface of the foam. The surface of MFC-SF crosslinked with 1.33% (wt/wt) PAEAPS-co-PDMS is comparatively smooth and non-gelatinized starch particles are visible. However, they spread on the surface of the foam sheet but formed small gaps between the spread gelatinized and non-gelatinized starch



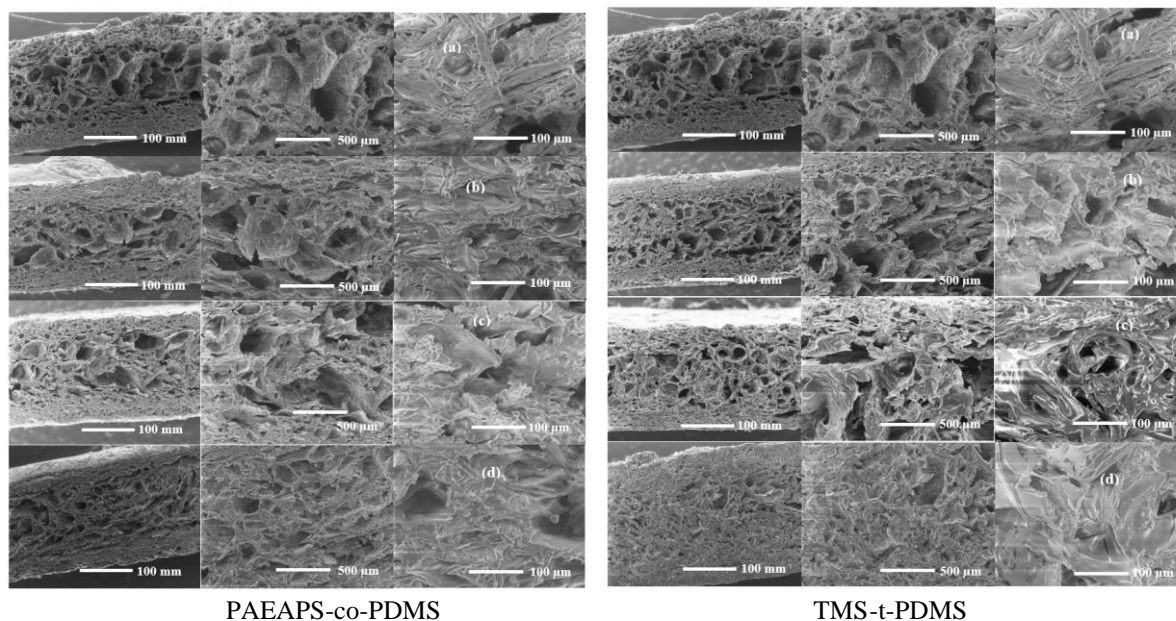


**Fig. 6.** SEM micrographs of neat (top) and cracked (bottom) surfaces of control MFC-SF (a) and also MFC-SFs crosslinked with 1.33 (b), 2.66 (c), and 5.32 (d)% (wt/wt) PAEAPS-co-PDMS and TMS-t-PDMS.

particles. Some cellulose fibers are also visible, but they are strongly bonded with starch. With increasing the PAEAPS-co-PDMS concentration, the surface became smooth and the cellulose fibers are strongly bonded with the matrix starch polymer and no non-gelatinized starch particles are visible on the surface. In the case of TMS-t-PDMS, even at 1.33%, the MFC fibers are strongly bonded to the matrix starch polymer (Fig. 6). With the increase in the TMS-t-PDMS concentration, the deposition of the polymer on the foam surface is visible and at 5.32% (wt/wt) concentration, droplets of TMS-t-PDMS are visible, which shows that TMS-t-PDMS did not mix with the starch and cellulose homogeneously as good as PAEAPS-co-PDMS as the former is hydrophobic and the micellar size was also larger compared to the PAEAPS-co-PDMS.

The effect of crosslinking with PAEAPS-co-PDMS and TMS-t-PDMS on the morphologies of the MFC-SFs was examined by SEM scanning of their cracked surfaces. Compared to the control MFC-SFs, the MFC-SFs crosslinked with polysiloxanes showed quite different morphologies. In the case of MFC-SF control, the area near both surfaces of the foam was also porous with small pores and in the middle larger pores. In the case of crosslinked MFC-SFs, the area near both surfaces was almost non-porous, and the size and the density of the pores were much smaller compared to the control. At 5.32% of the TMS-t-PDMS, the pore density considerably decreased. The morphology of the MFC-SFs crosslinked with both polymeric siloxane crosslinking agents was quite similar.

### 3.6. Dynamic contact angle

Table 3 shows the dynamic contact angle of MFC-SFs crosslinked with various concentrations of PAEAPS-co-PDMS and TSM-t-PDMS. The control MFC-SF showed some level of hydrophobicity because of the presence of carnauba wax, and hydrogen bond formation between hydroxyl groups of cellulose and starch but the contact angle gradually decreased with time. The contact angle produced by the surface of non-crosslinked MFC-SF

#### **Table 3.**

The dynamic contact angle of the surface of MFC-SFs crosslinked with reactive polysiloxane crosslinking agents.

Sample ID.	Average contact angle (°) at
------------	------------------------------

	0 s	120 s	240 s	360 s	480 s
Control	102.3±0.3	100.2±0.5	98.7±0.7	95.3±0.4	93.4±0.5
1.33% PAEAPS-co-PDMS	113.5±0.5	112.0±0.4	112.0±0.5	111.8±0.3	111.5±0.5
2.66% PAEAPS-co-PDMS	113.2±0.3	113.5±0.7	112.6±0.4	112.5±0.6	112.5±0.3
5.32% PAEAPS-co-PDMS	118.5±0.9	119.5±1.1	118.8±0.7	118.6±0.4	118.2±0.5
1.33% TMS-t-PDMS	117.8±0.3	115.4±0.3	115.4±0.6	115.4±0.4	115.8±0.6
2.66% TMS-t-PDMS	121.4±0.5	120.6±0.7	117.7±0.7	118.4±0.5	118.3±0.5
5.32% TMS-t-PDMS	122.9±0.3	121.5±0.7	120.3±0.5	120.8±0.6	120.6±0.5

at 0 s was 102.3°, which decreased to 93.4° after 480 s. The MFC-SF crosslinked with 1.33% (w/w) PAEAPS-co-PDMS exhibited better hydrophobicity than the control MFC-SF and the contact angle was comparatively stable over time. The contact angle shown by this sample at 0 s was 113.2°, which decreased to 112.5° at 480 s. The hydrophobicity of the MFC-SFs increased with an increase in the concentration of PAEAPS-co-PDMS and at 5.32% (wt/wt) PAEAPS-co-PDMS, the contact angle increased to 118.5°, which decreased to only 118.2° after 480 s. The MFC-SFs crosslinked with TSM-t-PDMS showed slightly better hydrophobicity compared to MFC-SFs crosslinked with PAEAPS-co-PDMS. The contact angle showed by the MFC-SF crosslinked with 1.33% TSM-t-PDMS exhibited a contact angle almost similar to the contact angle exhibited by the MFC-SF crosslinked with 5.32% PAEAPS-co-PDMS but the contact angle until 480 s. The highest contact angle was shown by the composite crosslinked with 5.32% (w/w) TSM-t-PDMS, as the contact angle after 480 s was still 120.6°. Overall, the MFC-SFs crosslinked with reactive polysiloxanes exhibited much better hydrophobicity compared to the MFC-SFs crosslinked with citric acid [10]. The dynamic contact angle data suggest that the crosslinking considerably increased the surface hydrophobicity of the MFC-SFs, which is consistent with the increase in the surface contact angle of the citric acid crosslinked starch/cellulose composite foams.

### 3.7. EDX spectra and elemental analysis

Fig. 7 shows the EDX spectra of MFC-SFs crosslinked with PAEAPS-co-PDMS and TMS-t-PDMS. The EDX spectrum of control MFC-SF does not show any presence of silicone peak, but all the crosslinked MFC-SFs show silicone peak. As expected, the intensity of the silicone peak increased with an increase in the weight% of reactive polysiloxane crosslinking agents.

Table S1 (Supplementary material) shows the C, O, and Si elemental analysis of the surface of MFC-SFs crosslinked with two trimethylsiloxy containing polysiloxane polymers. The Si content for the control MFC-SF was 0 as no silicone compound was present in the control MFC-SF. In the case of PAEAPS-co-PDMS, Si content proportionally increases with an increase in the PAEAPS-co-PDMS concentration. However, the Si content in the TMS-t-PDMS crosslinked MFC-SFs was considerably higher than the PAEAPS-co-PDMS crosslinked MFC-SFs. PAEAPS-co-PDMS is a copolymer compared to the TMS-t-PDMS, and therefore the Si content in the MS-t-PDMS crosslinked MFC-SFs was higher than the Si content of the PAEAPS-co-PDMS crosslinked MFC-SFs.

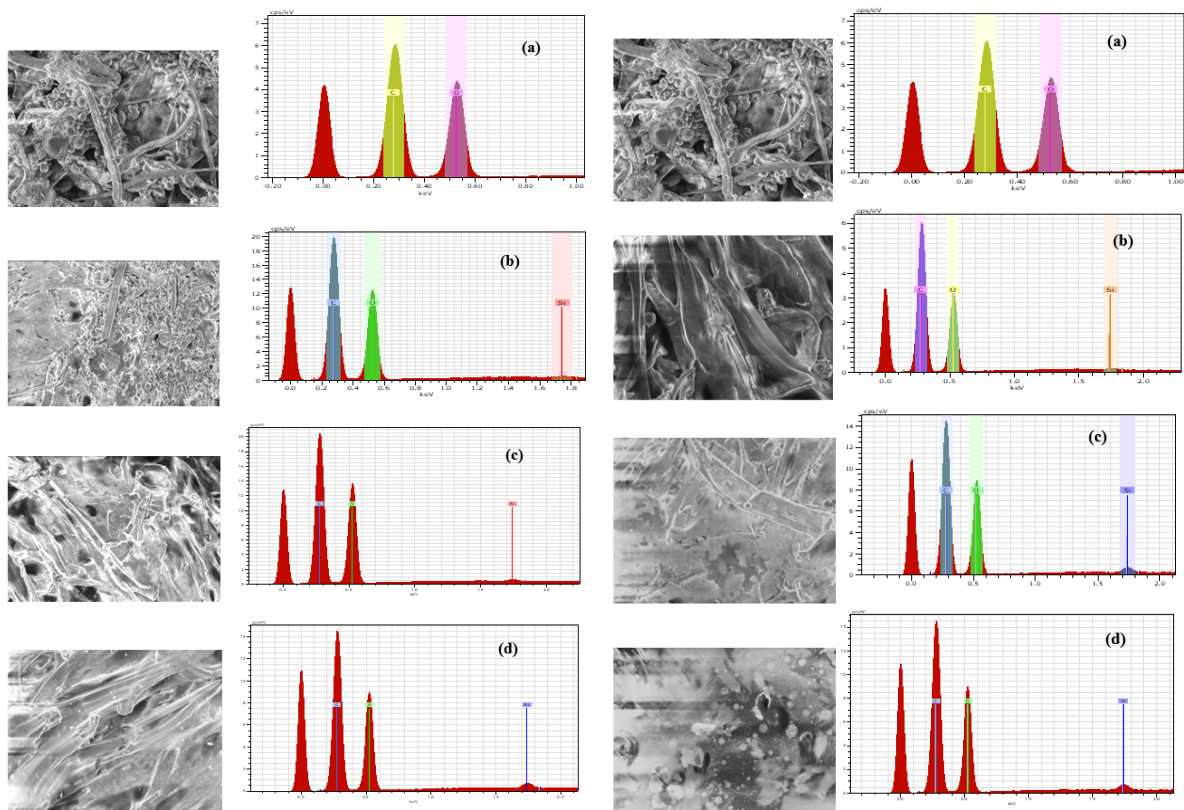


**Fig. 7.** EDX spectra of control MFC-SF (a) and also MFC-reinforced starch foams crosslinked with 1.33 (b), 2.66 (c), and 5.32 wt% (d) of PAEAPS-co-PDMS (left) and TMS-t-PDMS (right).

The elemental distribution of C, O, and Si on the surface of MFC-SFs crosslinked with various concentrations of PAEAPS-co-PDMS and TMS-t-PDMS is presented in Figs. S6 and S7 (Supplementary Material) respectively. It is evident that all the elements, especially the silicone are evenly distributed on the surface of crosslinked MFC-SFs. However, in the case of TMS-t-PDMS, Si is less uniformly distributed compared to the Si in the PAEAPS-co-PDMS crosslinked MFSC-SFs suggesting some level of incompatibility of the TMS-t-PDMS with cellulose and starch.

### 3.8. ATR-FTIR

Fig. S8 (Supplementary Materials) shows the ATR-FTIR spectra of control MFC-SF and also the MFC-SFs crosslinked with various concentrations of PAEAPS-co-PDMS and TMS-t-PDMS. The ATR-FTIR spectrum of non-crosslinked MFC-SF shows characteristic IR bands of starch and cellulose at 758, 847, 930, 992, 1014, 1078, 1150, 1249, 2849, 2917, and a broad IR band at 3255  $\text{cm}^{-1}$ . The IR bands shown between 980 and 1160  $\text{cm}^{-1}$  (992, 1014, and 1078  $\text{cm}^{-1}$ ) are due to the C–O bond stretching band attributed to primary alcohols [32]. The band at 1150  $\text{cm}^{-1}$  can be assigned to the C–O–C asymmetric stretching vibrations, which shows that ether bonds were formed between the primary alcohol groups of starch resulting in a decrease in hydrophilicity. Therefore, the surface of the control starch/cellulose showed some level of hydrophobicity in the contact angle measurement (Table 3). The bands at 2849 and 2917  $\text{cm}^{-1}$  are due to symmetric and asymmetric C–H stretching vibrations. The broad IR band at 3255  $\text{cm}^{-1}$  can be attributed to hydroxyl groups of starch and cellulose. The ATR-FTIR spectra of crosslinked starch/cellulose composites also showed similar bands but the intensity of the hydroxyl band at 3255  $\text{cm}^{-1}$  decreased with an increase in the concentration of PAEAPS-co-PDMS indicating increased hydrophobicity, which is consistent with the dynamic contact angle data shown in Table 3. The hydroxyl band intensity in the case of TMS-t-PDMS-crosslinked-MFC-SFs was smaller compared to the hydroxyl band intensity of PAEAPS-co-PDMS crosslinked MFC-SFs suggesting that the TMS-t-PDMS crosslinking produced more hydrophobic surface compared to the surface produced by the PAEAPS-co-PDMS crosslinking, which is also consistent with the dynamic contact angle data of the MFC-SFs.

#### **4. Conclusions**

The MFC-SFs were crosslinked with two different reactive polysiloxane crosslinking agents that not only considerably increased the tensile strength and elongation but also enhanced the water barrier properties by enhancing the hydrophobicity and decreasing the water absorption capacity of the MFC-SFs. The density of the foam increased with an increase in the weight% of the PAEAPS-co-PDMS and TMS-t-PDMS, and the MFC-SFs crosslinked with TMS-t-PDMS showed slightly higher density compared to the foams crosslinked with PAEAPS-co-PDMS. The chemical crosslinking with elastomeric polysiloxane polymers decreased the stiffness of the prepared foams but had a marginal effect on the thermal stability of the starch foams. The crosslinking with PAEAPS-co-PDMS provided better tensile strength but the TMS-t-PDMS crosslinking provided better water barrier properties. The increase in crosslinking agent concentration decreased the stiffness, flexural rigidity, and water absorption capacity but increase the tensile strength and water barrier properties. FTIR analysis shows that the intensity of hydroxyl peaks decreased after the crosslinking reducing the hydrophilicity of the produced starch foams. This work demonstrates that polysiloxane crosslinked MFC-SFs has the potential to replace expanded polystyrene foam packaging used in the supermarket.

#### **Author contributions**

M.M. Hassan planned and carried out the work, and also wrote the article. I. Fowler carried out several testing and analyzed the data.

## Acknowledgment

The authors acknowledge the financial support received from Kiwi Innovation Network Limited and AgResearch Limited (Contract # A25410) to conduct this research. I would like to thank Hanh Nguyen (Food Science and Technology team, AgResearch) for measuring the micelle size of the polysiloxane emulsions, Mark Staiger (Department of Mechanical Engineering, University of Canterbury) for the DMTA analysis, and Chris Lepper (School of Chemical and Physical Sciences, Victoria University Wellington) for TG analysis.

## References

- [\*] K. Wang, L. Yang, M. Kucharek, Investigation of the effect of thermal insulation materials on packaging performance, *Packaging Technol. Sci.* 33 (2020) 227–236.
- [2] A. Castiglioni, L. Castellani, G. Cuder, S. Comba, Relevant materials parameters in cushioning for EPS foams, *Colloid. Surf. A* 534 (2017) 71–77.
- [3] A. Tinti, A. Tarzia, A. Passaro, R. Angiuli, Thermographic analysis of polyurethane foams integrated with phase change materials designed for dynamic thermal insulation in refrigerated transport, *Appl. Thermal Eng.* 70 (2014) 201–210.
- [4] M. Urgun-Demirtas, D. Singh, K. Pagilla, Laboratory investigation of biodegradability of a polyurethane foam under anaerobic conditions, *Polym. Degrad. Stab.* 92 (2007) 1599–1610.
- [5] T. Jiang, Q.-F. Duan, J. Zhu, H.-S. Liu, L. Yu, Starch-based biodegradable materials: Challenges and opportunities, *Adv. Ind. Eng. Polym. Res.* 3 (2020) 8–18.

- [6] G.M., Ganjyal, N., Reddy, Y.Q., Yang, M.A. Hanna, Biodegradable packaging foams of starch acetate blended with corn stalk fibers. *J. Appl. Polym. Sci.* 93 (2004) 2627–2633.
- [7] H.A. Pushpadass, G.S. Babu, R.W. Weber, M.A. Hanna, Extrusion of starch-based loose-fill packaging foams: Effects of temperature, moisture, and talc on physical properties, *Packaging Technol. Sci.* 21 (2008) 171–183.
- [8] C.M. Machado, P. Benelli, I.C. Tessaro, Sesame cake incorporation on cassava starch foams for packaging use, *Ind. Crop. Prod.* 102 (2017) 115–121.
- [9] J.B. Engel, A. Ambrosi, I.C. Tessaro, Development of biodegradable starch-based foams incorporated with grape stalks for food packaging, *Carbohydr. Polym.* 225 (2019) 115234.
- [\*0] M.M. Hassan, N. Tucker, M.J. Le Guen, Thermal, mechanical and viscoelastic properties of citric acid-crosslinked starch/cellulose composite foams, *Carbohydr. Polym.* 230 (2020) 115675.
- [\*1] P.R. Salgado, V.C. Schmidt, S.E. Molina Ortiz, A.N. Mauri, J.B. Laurindo, Biodegradable foams based on cassava starch, sunflower proteins, and cellulose fibers obtained by a baking process, *J. Food Eng.* 85 (2008) 435–443.
- [\*2] L.R.P.F. Mello, S. Mali, Use of malt bagasse to produce biodegradable baked foams made from cassava starch, *Ind. Crop. Prod.* 55 (2014) 187–193.
- [\*3] A. Ghanbari T. Tabarsa, A. Ashori, A. Shakeri, M. Mashkour, Thermoplastic starch foamed composites reinforced with cellulose nanofibers: Thermal and mechanical properties, *Carbohydr. Polym.* 197 (2018) 305–311.
- [\*4] Y. Srisuwan, Y. Baimark, Improvement of water resistance of thermoplastic starch foams by dip-coating with biodegradable polylactide-b-polyethylene glycol-b-polylactide copolymer and its blend with poly(D-lactide), *Prog. Org. Coat.* 151 (2021) 106074.

- [\*5] M.M. Hassan, M.J. Le Guen, N. Tucker, K. Parker, Thermo-mechanical, morphological and water absorption properties of thermoplastic starch/cellulose composite foams reinforced with PLA, *Cellulose* 26 (2019) 4463–4478.
- [\*6] J. Muller, C. González-Martínez, A. Chiralt, Combination of poly(lactic) acid and starch for biodegradable food packaging, *Materials* 10 (2017) 952.
- [\*7] H. Yavuz, C. Babaç, Preparation and biodegradation of starch/polycaprolactone films, *J. Polym. Environ.* 11 (2003) 107–113.
- [\*8] Q. Fang, M.A. Hanna, Functional properties of polylactic acid starch-based loose-fill packaging foams, *Cereal Chem.* 77 (2000) 779–783.
- [\*9] K. El-Tahlawy, R.A. Venditti, J.J. Pawlak, Aspects of the preparation of starch microcellular foam particles crosslinked with glutaraldehyde using a solvent exchange technique, *Carbohydr. Polym.* 67 (2020) 319–331.
- [20] I. Gonenc, F. Us, Effect of glutaraldehyde crosslinking on degree of substitution, thermal, structural, and physicochemical properties of corn starch, *Starch* 71 (2019) 1800046.
- [2\*] P. Yin, X. Dong, W. Zhou, D. Zha, J. Xu, B. Guo, P. Li, A novel method to produce sustainable biocomposites based on thermoplastic corn-starch reinforced by polyvinyl alcohol fibers, *RSC Adv.* 10 (2020) 23632–23643.
- [22] M.-K. Uslu, S. Polat, Effects of glyoxal cross-linking on baked starch foam, *Carbohydr. Polym.* 87 (2012) 1994–1999.
- [23] Z. Iqbal, W. Moses, S. Kim, E.J. Kim, W.H. Fissell, S. Roy, Sterilization effects on ultrathin film polymer coatings for silicon-based implantable medical devices, *J. Biomed. Mater. Res. B* 106 (2018) 2327–2336.

- [24] J. Stieghorst, D. Majaura, H. Wevering, T. Doll, Toward 3D printing of medical implants: reduced lateral droplet spreading of silicone rubber under intense IR curing, *ACS Appl. Mater. Interf.* 8 (2016) 8239–8246.
- [25] T. Aziz, M. Waters, R. Jagger, Analysis of the properties of silicone rubber maxillofacial prosthetic materials, *J. Dent.* 31 (2003) 67–74.
- [26] L.A. Ramos, E. Frollini, A. Koschella, Th. Heinze, Benzylation of cellulose in the solvent dimethylsulfoxide/tetrabutylammonium fluoride trihydrate, *Cellulose* 12 (2005) 607–619.
- [27] S.-J. Jiang, T. Zhang, Y. Song, F. Qian, Y. Tuo, G. Mu, Mechanical properties of whey protein concentrate based film improved by the coexistence of nanocrystalline cellulose and transglutaminase, *Int. J. Biologic. Macromol.* 126 (2019) 1266–1272.
- [28] A.T. Paulino, J.I. Simionato, J.C. Garcia, J. Nozaki, Characterization of chitosan and chitin produced from silkworm chrysalides, *Carbohydr. Polym.* 64 (2006) 98–103.
- [29] C. White, K. Tan, A. Wolf, L. Carbary, Advances in structural silicone adhesives, in: D.A. Dillard (ed.), *Advances in Structural Adhesive Bonding*, Woodhead Publishing, 2010. pp. 66–95.
- [30] Y. Tian, Y. Li, X. Xu, Z. Jin, Starch retrogradation studied by thermogravimetric analysis (TGA), *Carbohydr. Polym.* 84 (2011) 1165–1168.
- [31] I. Šmkovic, E. Jakab, Thermogravimetry/mass spectrometry study of weakly basic starch-based ion exchanger, *Carbohydr. Polym.* 45 (2001) 53–59.
- [32] Y. Maréchal, H. Chanzy, The hydrogen bond network in I( $\beta$ ) cellulose as observed by infrared spectrometry, *J. Mol. Struct.* 523 (2000) 183–196.